Biomechanics of Joints and Orthopaedic Implants
Professor. Sanjay Gupta
Department of Mechanical Engineering
Indian Institute of Technology, Kharagpur
Lecture 35
Bone Remodelling Around Resurfaced Femur and Pelvic Bone

Good afternoon everybody. Welcome to the second lecture in the seventh module on Bone Remodeling around Resurfaced Femur and Pelvic Bone.

(Refer Slide Time: 0:43)

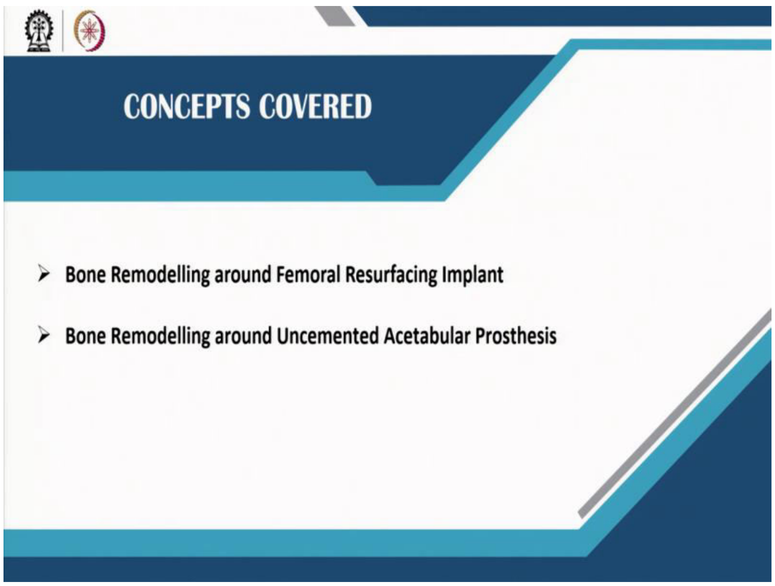

Now in this lecture, we will be discussing the bone remodeling around femoral resurfacing implant. And we will also be discussing about bone remodeling around uncemented acetabular Prosthesis.

(Refer Slide Time: 1:04)

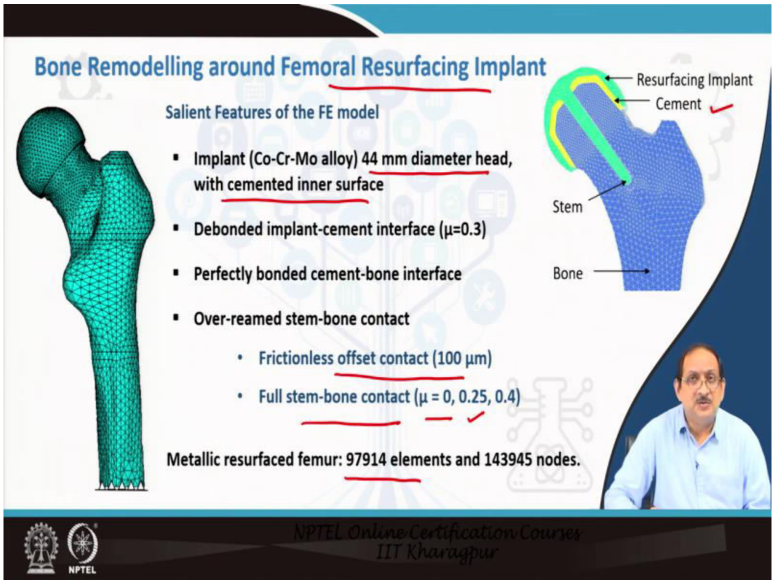

Let us consider the first topic that is bone remodeling around femoral resurfacing implant. Now, we have discussed about it earlier. So, let me summarize the salient features of the finite element model of the resurfaced femur. So, the implant used is a metallic implant, cobalt-chrome-molybdenum alloy and it is 44-millimeter diameter head, and it is cemented in the inner surface as indicated here.

So, the resurfacing implant is shown here in the coronal section, the green portion, and the yellow portion is the cement which is located in the inner surface of the resurfacing implant. Now, we have used debonded implant cement interface having friction coefficient of 0.3 in the finite element model. Now, the cement bone interface is assumed to be perfectly bonded. However, the stem goes inside an over-reamed hole in the proximal femur.

So, there is a variable stem bone contact condition. So, it can be frictionless offset contact having a gap of 100 microns, and it can also be a full stem bone contact. It may be frictionless, it may be μ equal to 0.25, or the friction coefficient maybe 0.4. Now, the metallic resurfaced femur finite element model consisted of about 100,000 elements and this model was developed based on the CT scan data set of a subject.

So, the bone elements within the implant-bone structure was assigned individual bone material properties using the linear calibration and the power-law density modulus relationship as discussed in detail earlier.

(Refer Slide Time: 3:50)

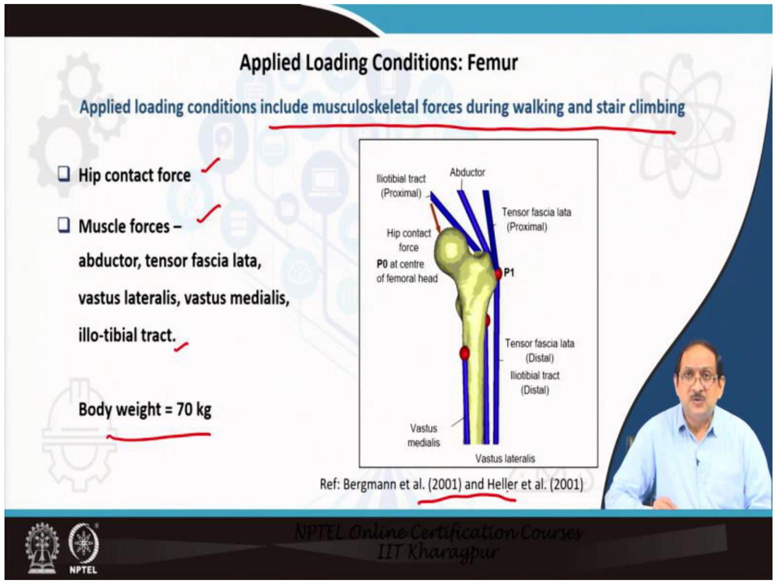

The applied loading conditions used for the analysis include the musculoskeletal forces during walking and stair climbing. Now, this set of musculoskeletal forces consists of the hip contact force and the muscle forces such as the abductor, tensor fascia lata, vastus lateralis, vastus medialis, and illio-tibial tract. The bodyweight of the subject was assumed to be 70 kilogram and the musculoskeletal model of forces or the data was obtained from the hip 98 data set.

(Refer Slide Time: 4:44)

Now, let us discuss about some serious complications and failure mechanisms of the hip resurfacing arthroplasty. Now, clinical studies reported femoral neck fracture as the most common short-term failure mechanism. So, the femoral neck fracture is regarded as the most common short-term failure mechanism.

Moreover, in the long-term, stress and strain shielding, as well as adverse bone remodeling, eventually caused implant loosening. Now, in the figure presented here, you can see that there is a black line in the X-ray from the proximal femoral neck region progressing further and causing the total femoral neck fracture. And this actually has happened a few months after the surgery.

(Refer Slide Time: 6:10)

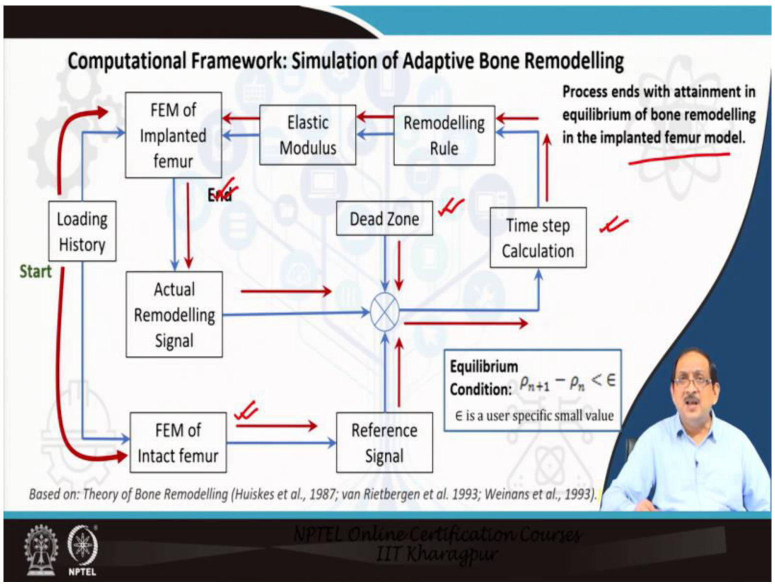

Now, we have set out to investigate the biomechanical causes that may be responsible for the failure in hip resurfacing arthroplasty. So, we are using the computational framework, a simulation of adaptive bone remodeling as discussed earlier. So, as you know that this framework is based on the theory of bone remodeling and it starts with the development of the finite element model of intact femur and implanted femur.

Now, we apply loading conditions to each model: the intact femur model and the implanted femur model and we calculate the reference signal or the reference stimulus and we calculate the remodeling stimulus of the remodeling signal. Now, after calculating these two mechanical stimuli, we can compare it with the dead zone, and if the values fall beyond the dead zone, then for the bone element, the remodeling process starts.

So, it starts with the time step calculation. Thereafter, we can apply the remodeling rule, and we can calculate an updated value of the bone density leading to an updated value of the bone

Young's modulus. So, a new or updated material model of the FE model of the implanted femur is obtained, and this cycle goes on iteratively until we reach an end with the attainment of equilibrium of bone remodeling in the implanted femur model.

The equilibrium condition is satisfied when the difference in the successive values of bone density is less than a user-specified small value.

(Refer Slide Time: 8:43)

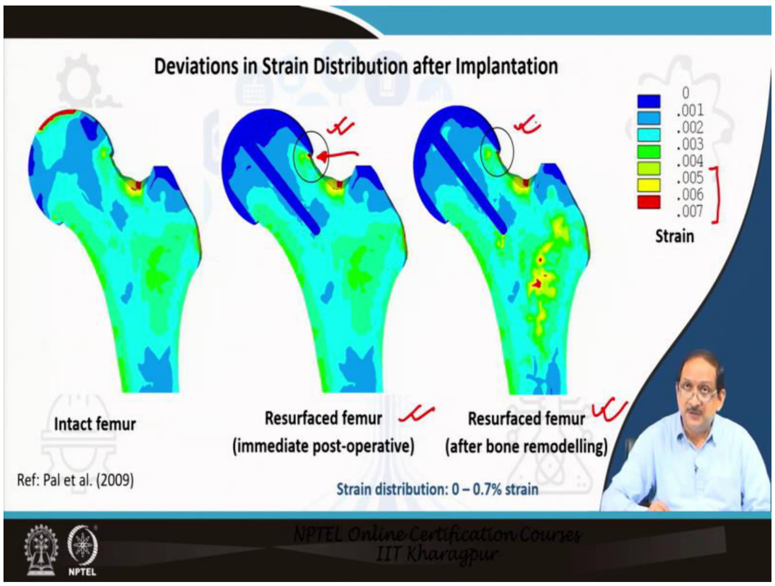

Now, let us come to the results. As you can see here that I have presented this strain distribution in the intact femur and the strain distribution is plotted from 0 to 0.7 percent strain. Now, the second figure presented now is the strain distribution corresponding to immediate post-operative condition. So, here we see that postoperatively, substantial strain shielding that is reduction in strain of around 20 percent to 70 percent as compared to the intact femur was observed inside the proximal femoral head.

The resurfacing procedure leads to elevated strains in the range of 0.5 percent to .7 percent strain around the proximal femoral neck region, in particular around the proximal neck implant junction, as indicated by the black circle here in the figure. Now, this occurs irrespective of variation of the strain bone contact condition.

Now, this strain concentration and the magnitude of the elevated strain, is very close to the yield strain of femoral neck cancellous bone, which is around 0.6 to 0.7 percent strain. Clinical studies reported that one of the major concerns of hip resurfacing arthroplasty is the risk of femoral neck fracture during the first two to three months after surgery.

This strain concentration generated postoperatively at the proximal femoral neck region as indicated by the arrow indicates a potential risk of neck fracture. However, with bone remodeling, these strain concentrations actually disappear.

(Refer Slide Time: 11:29)

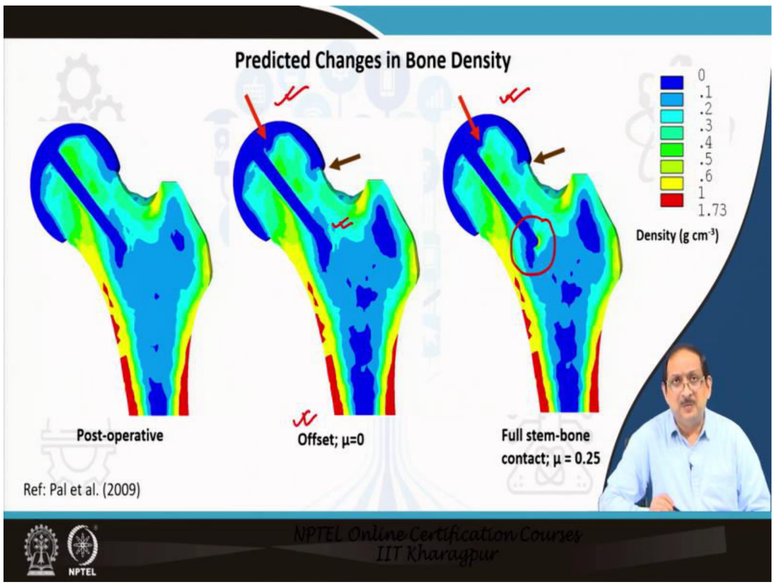

Now, let us now look into the predicted changes of bone density. Now strain shielding led to adverse bone remodeling within the resurfaced femoral head. Now changes in bone density pattern were influenced by the stem bone condition. The differences in predicted bone density around the prosthesis were influenced by the stem bone contact condition, although the patterns of predicted changes in bone density were roughly similar.

Now bone density reductions of 50 to 80 percent as compared to the intact femur were observed in the regions underlying the resurfaced head, indicating severe bone resorption. So, bone density reductions of about 50 to 80 percent as compared to the intact femur were calculated in the case of the resurfaced femur irrespective of the stem bone contact condition.

But one point to note here in the figure, as you can see towards the distal tip of the stem. When the stem is in contact with the surrounding bone, we observed some bone opposition or increase in bone density around the distal tip of the stem as compared to the offset condition where there is hardly any contact between the stem and the surrounding bone. Hence, there is no bone apposition or no hardly any change in the bone density around the distal tip of the stem.

(Refer Slide Time: 14:01)

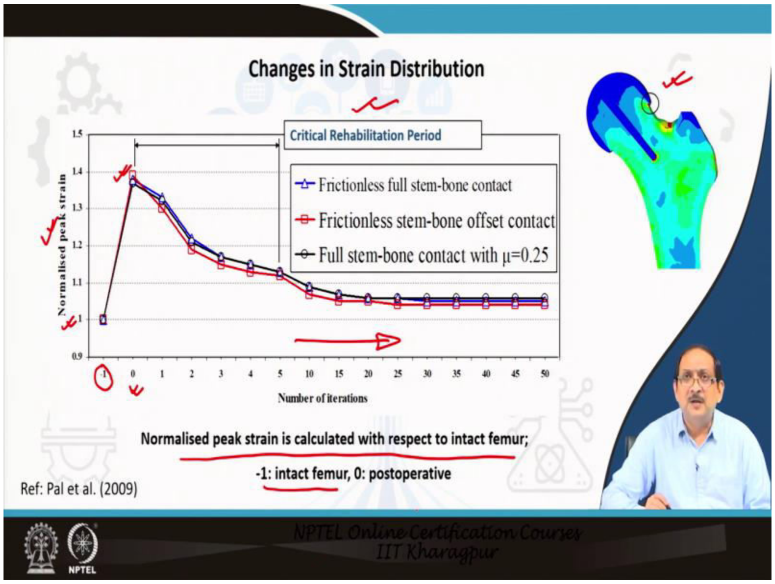

Let us now discuss about the changes in strain distribution after surgery and the progression of bone remodeling. Now, the figure presents the increase in strain in the proximal femoral neck region. So, we are interested in a critical appreciation of the proximal femoral neck region, the bone elements located in that region. So, in this figure, we present the normalized peak strain, which is calculated with respect to the intact femur.

That means that in the intact condition i.e. pre-operative condition, the normalized peak strain is equal to 1. The condition corresponding to 0 number of iteration is the immediate post-operative condition. And you can see that the normalized peak strain has increased to about 1.4 times that of the intact femur indicating a risk of femoral neck fracture during early post-operative period, designated as the critical rehabilitation period in the figure.

It should, however, be noted that this strain concentration was considerably reduced with bone remodeling, thereby lowering the risk of femoral neck fracture over time. It should also be noted that the stem bone interface condition had minimal effect on the normalized peak strain postoperatively and with progression in bone remodeling.

(Refer Slide Time: 16:28)

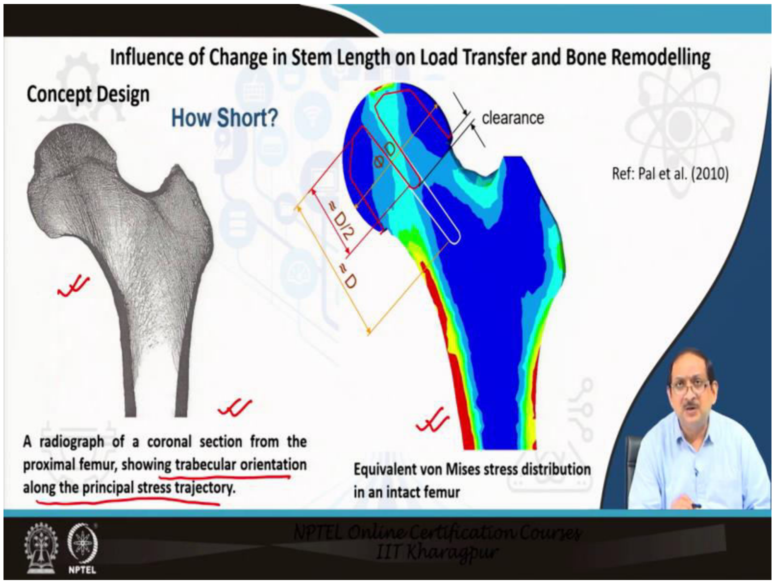

Now, let us consider the influence of changing stem length on load transfer and bone remodeling. Now, as you can see here, the figure on the left presents a radiograph of a coronal section of the proximal femur showing trabecular orientation along the principal stress trajectory.

Now, based on this natural stress distribution, as you can see in the case of an intact femur, the Von Mises stress distribution presented here in the slide is actually quite similar to the trabecular orientation presented here in the radiograph. We intended to change the stem length in order to obtain a stress distribution or strain distribution very similar to the intact condition. So, we set out with the concept design.

But the main question that needs to be addressed is if you want to reduce the stem length to alter the stress-strain distribution within the resurfaced femur, then how short will be the stem length. Now, here is the concept, which is represented by the long stem, which is marked by the white-colored stem and the red stem, and you can see that the stem length has been reduced to half the original length.

Now, the stem length is equal to the radius of the resurfacing head. Earlier in the long stem case, the length of the stem was equal to the diameter of the resurfaced head.

(Refer Slide Time: 19:01)

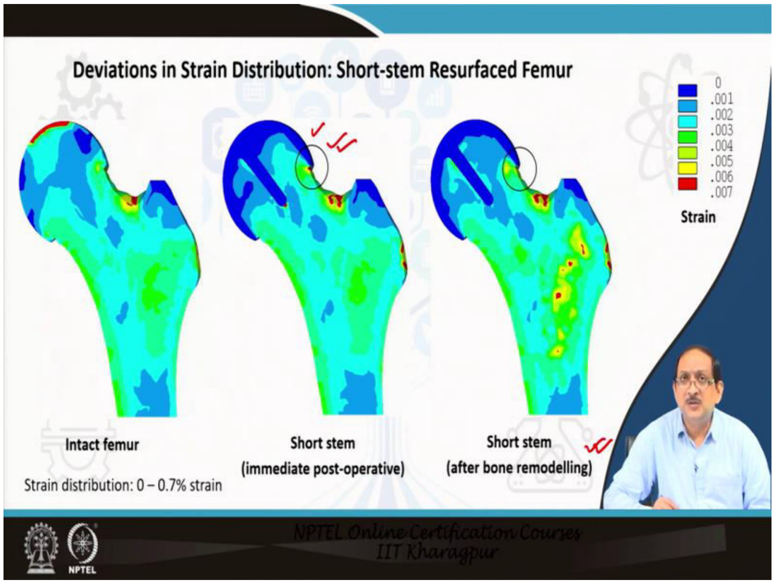

Let us now look into the deviations in the strain distribution for the short stem resurfaced femur. Now, shortening the stem length to half the current length leads to more physiological strain distribution, as is evident from the figure. This actually led to the reduced effect of strain shielding, reduction of strain concentration around the proximal femoral neck region and the distal tip of the stem.

Now, whatever be the increase in the peak strain around the proximal femoral neck region, Similar to the long stem, this elevated strain actually was reduced to a great extent with bone remodeling. In the case of the short stem design, the occurrence of elevated strains in the proximal femoral neck implant junction is evident, which actually reduces with bone remodeling.

(Refer Slide Time: 20:48)

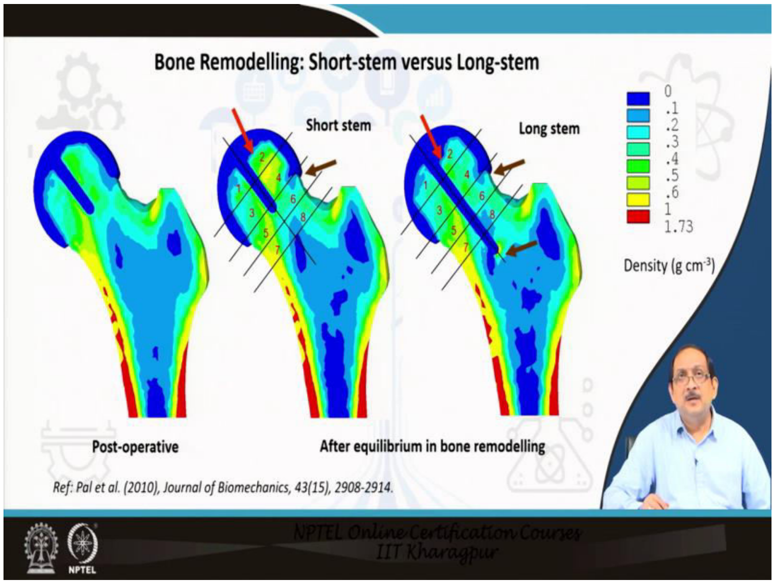

Now, let us present to you the short stem versus the long stem. And in this figure, it is evident that the short stem provides a far more physiological stress distribution as compared to the long stem, as indicated by the reduced effect of bone remodeling in the regions as indicated in the slide.

(Refer Slide Time: 21:34)

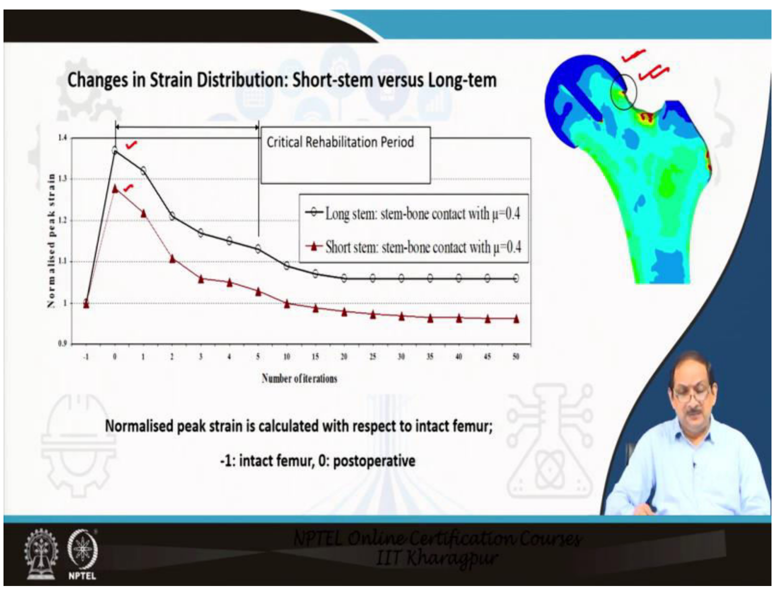

Now, let us compare the normalized peak strain in the proximal femoral neck region from where the fracture is expected to be initiated. We see that in the case of short stem, the normalized peak strain reduces to about 1.28 times that of the intact femur compared to 1.4 times in the case of the long stem. Now, this elevated strain in this region, the proximal femoral neck region, is reduced with bone remodeling, as indicated in the slide.

(Refer Slide Time: 22:39)

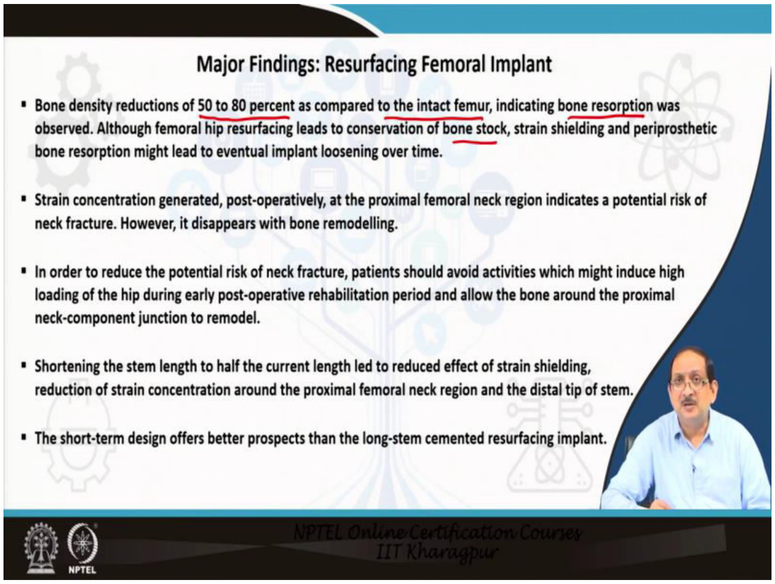

Let us now summarize the major findings of the resurfacing femoral implant. Bone density reductions of 50 to 80 percent as compared to the intact femur indicating bone resorption was observed. Although femoral hip resurfacing leads to conservation of bone stock, strain shielding and periprosthetic bone resorption might lead to eventual implant loosening over time. Strain concentration generated postoperatively at the proximal femoral neck region indicates a potential risk of neck fracture.

However, it disappears with bone remodeling. In order to reduce the potential risk of neck fracture, patients should avoid activities that might induce high loading of the hip during early post-operative rehabilitation period and allow the bone around the proximal neck component junction to remodel.

Shortening the stem length to half the current length leads to reduced effect of strain shielding, reduction of strain concentration around the proximal femoral neck region and the distal tip of the stem. The short stem design, therefore, appears to offer better prospects than the long stem cemented resurfacing implant.

(Refer Slide Time: 24:26)

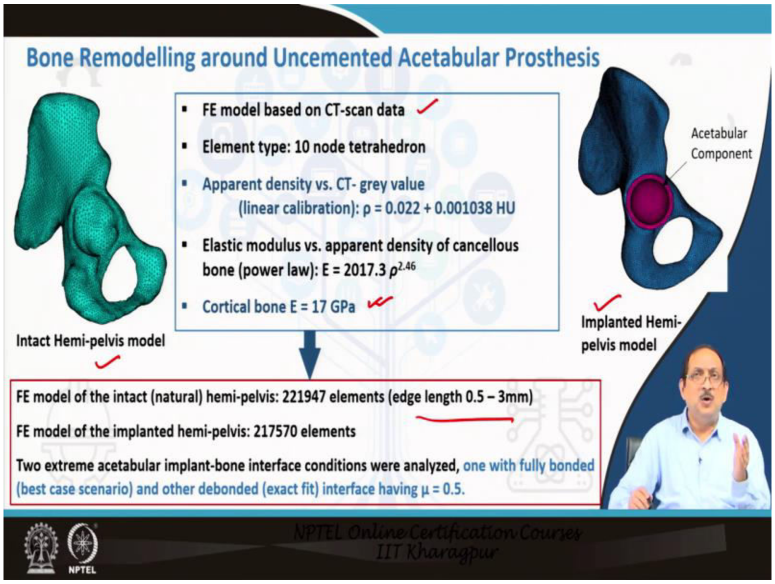

Let us now come to the second topic of this lecture, which is bone remodeling around the uncemented acetabular prosthesis. So, the finite element model of an intact hemi pelvis and an implanted hemi pelvis are based on CT scan data of a subject. Now, the element type used in this finite element model is ten noded tetrahedron.

The heterogeneous material properties of each bone element in the finite element model can be assigned individual material properties like apparent density and Young's modulus based on the relationships. The cortical bone is generally assigned 17 Giga Pascal value of Young's modulus. Now, the FE model of the intact hemi pelvis consisted of 221947 elements.

And the edge length of the elements vary between 0.5 millimeter to 3 millimeter. Whereas, finite element model of the implanted Hemi pelvis consisted of 217570 elements. Now, two extreme implant bone interface conditions were analyzed. Now, this is a uncemented prosthesis. So, the interface is the only interface is between the implant and the bone.

So, two conditions have been simulated: one with fully bonded that is regarded as the best case scenario, the implant is fixed to the bone and fully bonded to the bone. So, one is a fully bonded interface, and the other is a debonded interface having a friction coefficient equal to 0.5.

(Refer Slide Time: 27:05)

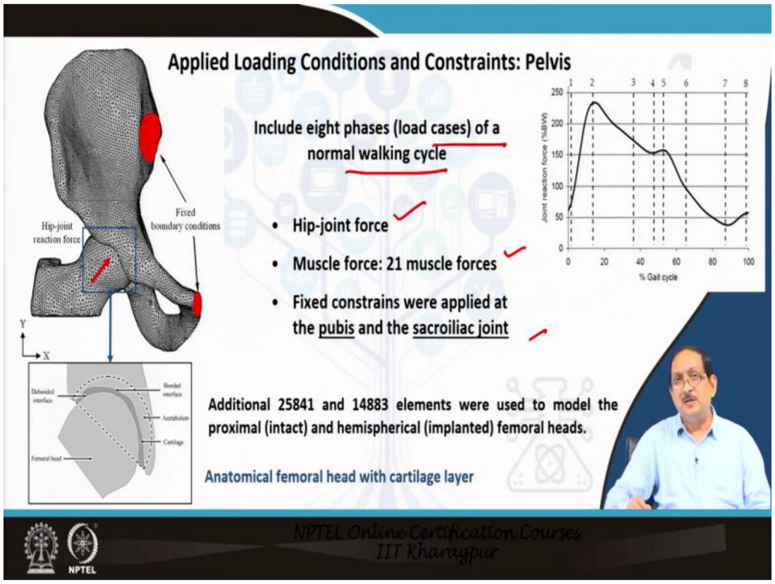

The applied loading conditions and constraints were discussed earlier as well, I am summarizing it in this slide. Now, the applied loading conditions included 8 phases or 8 load cases of a normal walking cycle. And the loading conditions or the load cases consisted of data on hip joint force 21 muscle forces and fixed constraints were prescribed at the pubis and sacroiliac joint. Now, we had actually applied the hip joint reaction force through the femoral head and a cartilage layer.

So, anatomical femoral head with a cartilage layer was included in the model mainly to apply the hip joint reaction force through the center of the femoral head. Therefore, an additional about 26,000 elements and around 15,000 elements were generated to model the proximal, that is the for the intact condition, the proximal femoral head, and for the hemispherical implanted femoral head.

(Refer Slide Time: 28:33)

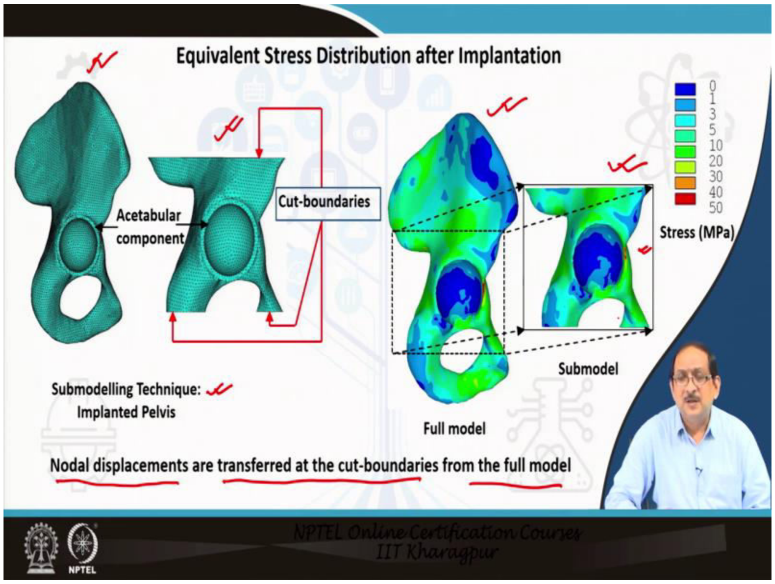

Now, as discussed earlier, we have employed this submodeling technique for the analysis of the finite element model of the implanted pelvis. Now, the objective of using a submodel with a fine mesh around the prosthesis or the domain of inclusion of the prosthesis is to focus our investigation in and around the inclusion of the acetabular component or the prosthesis.

Now, the elastic behavior of the remaining part of the pelvic bone as indicated in the full model of the pelvic bone with the prosthesis needs to be included in the submodel using the submodeling technique. So, the submodeling technique calls for nodal displacements to be transferred at the cut boundaries from the full model. The efficacy of this method has been checked by comparing the stress distribution in the full model with the stress distribution in the submodel.

As you can see in the figure, that the stress distribution in and around the acetabulum is almost similar, barring a few deviations in stresses as indicated here in the corner right corner of the acetabulum. Now, this occurs mainly because the submodel was meshed with a very fine mesh with very small elements. So, the description of the material properties is far more elaborate in the case of the submodel as compared to the full model.

And therefore this leads to small deviations in the quantitative values of peak stresses in and around that region.

(Refer Slide Time: 31:17)

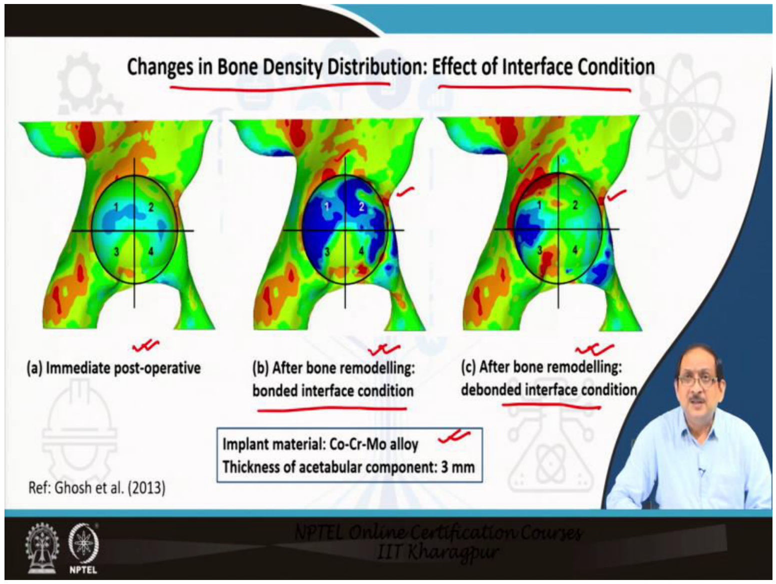

Let us now present to you the changes in bone density distribution considering the effect of implant-bone interface condition. The figure on the left presents the bone density distribution corresponding to the immediate post-operative scenario, which is basically corresponding to the intact bone condition. Now, after bone remodeling and considering the fully bonded interface condition, we observe a considerable effect of bone resorption in the central region of the implanted acetabulum.

There are, however, peripheral regions of increased bone density that is bone apposition basically located around the periphery of the acetabulum. Now, in the case of bone remodeling, when we simulate debonded implant-bone interface condition, we observed that there are regions of bone resorption, but the effect of bone resorption is less compared to the bonded implant-bone condition as indicated in figure c in regions 1 and 3.

Now, here also, we observed bone apposition around the periphery of the acetabulum. These results of changes in bone density distribution correspond to a metallic cobalt-chromium-molybdenum alloy, and the acetabular component has a thickness of 3 millimeter.

(Refer Slide Time: 33:39)

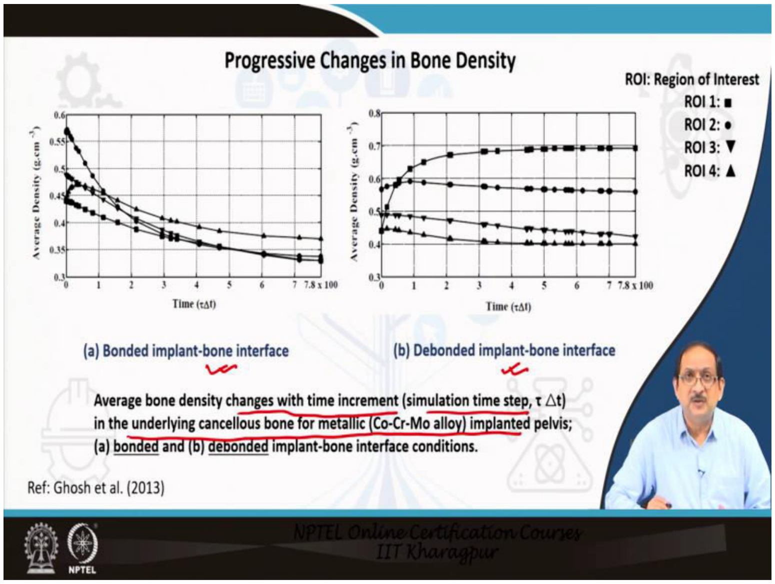

The progressive changes of bone density in these 4 regions of interest 1, 2, 3, 4 have been presented here in the slide. Now, the average bone density changes have been plotted against the simulation time step, which I had remarked in my earlier lecture in 7.1, an arbitrary timescale, in the underlying cancellous bone for the metallic acetabular component.

Now, here two interface conditions have been presented: one bonded implant-bone interface and other implant debonded implant-bone interface. And you can clearly differentiate between the progressive changes in bone density due to changes in implant-bone interface condition.

(Refer Slide Time: 34:48)

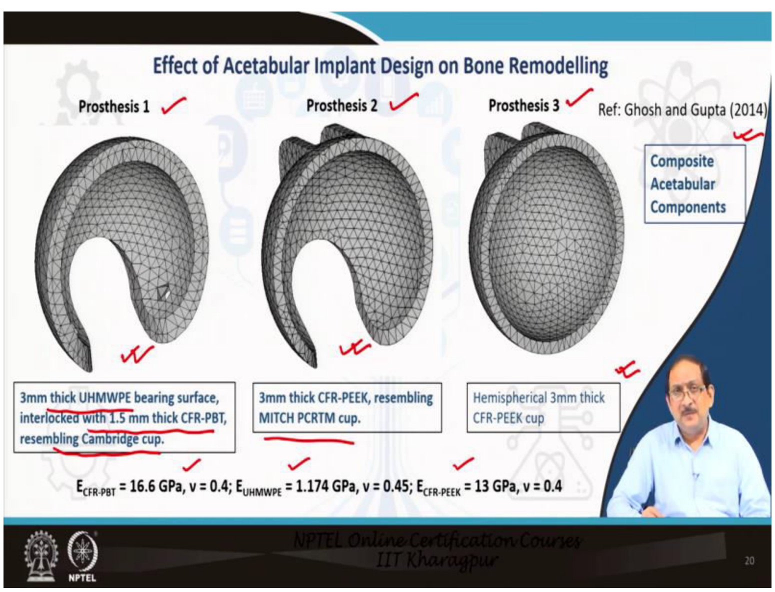

Let us discuss the effect of acetabular implant design on bone remodeling, and in this study, we have considered more flexible composite acetabular components basically made up of polymer composites. So, we have three designs: prosthesis 1, prosthesis 2, prosthesis 3 presented in the figure. The prosthesis 1 is actually resembling a Cambridge cup. It has a three-millimeter ultra high molecular weight polyethylene bearing surface interlocked with 1.5 millimeter thick CFR-PBT.

So, the total thickness of acetabular component is 4.5 millimeter. The prosthesis 2 resembles a MITCH cup and has a 3 millimeter thick CFR-PEEK component. And the prosthesis 3, as you can see here, has a fully hemispherical 3 millimeter thick CFR-PEEK Cup. It should also be noted that in the case of prosthesis 1 and prosthesis 2, there is a horseshoe shaped cutout, which is not present in the case of prosthesis 3.

So, what does that mean in terms of mechanics? It means that the rigidity of the implant or the stiffness of the implant varies in cases of prosthesis 1, 2 and 3 because the geometry of the prosthesis is changing. The E modulus of CFR-PBT ultra high molecular polyethylene and the CFR-PEEK is indicated here along with the Poison's ratio.

(Refer Slide Time: 37:15)

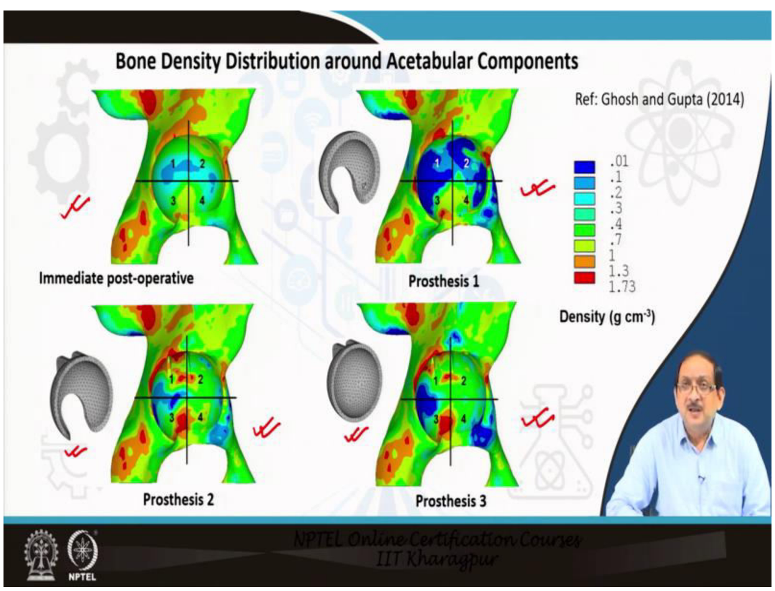

Now, let us compare the bone density distribution around these flexible acetabular components. Now, the first figure on the top left is the immediate post-operative scenario. The second figure on the top right corresponds to prosthesis 1, Cambridge cup. You can see that due to the 4.5 millimeter thick prosthesis, there is an appreciable amount of bone resorption in the central region of the acetabulum.

In case of prosthesis 2 that resembles a MITCH cup, bottom left, we have the minimum effect of bone resorption indicated by the blue color. In case of prosthesis 3, which is a hypothetical 3 millimeter peak hemispherical acetabular component, we see that the changes in density distribution due to bone remodeling is something in between prosthesis 1 and prosthesis 2.

So, it does show some amount of bone resorption but, the amount of bone resorption is less than the 4.5 millimeter thick prosthesis 1 because prosthesis 3 and prosthesis 2, both have 3 millimeter thickness CFR-PEEK component. However, in case of prosthesis 3, there is no cutout, thereby increasing the stiffness of the prosthesis.

(Refer Slide Time: 39:45)

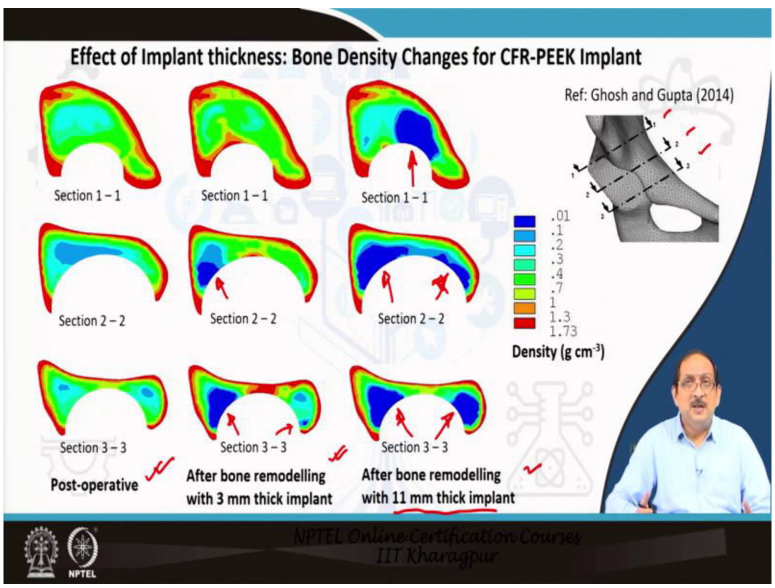

Now, when we look at sectional plots, it is pretty much evident, the changes in bone density due to the thickness of the implant. If we take three sections 1, 2, and 3 as indicated in the FE model of the acetabulum part or the FE model of the pelvic bone at three locations: superior, middle, and inferior. When we plot it on the left, we have the post-operative condition showing the distribution of the bone density; pre-operative or post-operative is the same.

Because now there is no bone remodelling setting in. After bone remodelling with 3 millimeter thick CFR-PEEK implant, we observe bone resorption, the presence of deep blue color in section

3-3 and section 2-2. When we use a 11 millimeter thick implant, please not that bone resorption is considerably increased in all the section, section 1-1, section 2-2, section 3-3. So, what does that mean, with an increase in thickness, the stiffness of the implant increases as well as the rigidity of the implant increases, Thereby, evoking more adverse bone remodelling in the underlying cancellous bone.

(Refer Slide Time: 41:44)

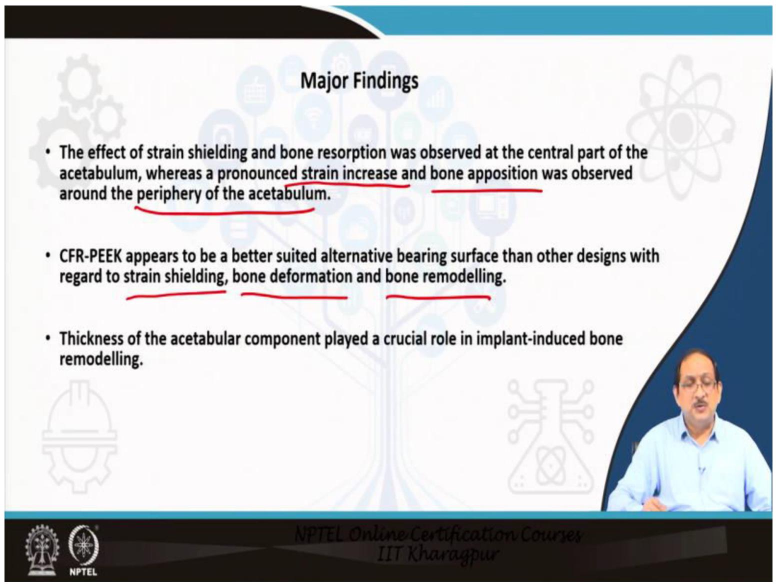

Let us summarize the major findings of the study. The effect of strain shielding and bone resorption was observed at the central part of the acetabulum, whereas a pronounced strain increase and bone apposition was observed around the periphery of the acetabulum. CFR-PEEK appears to be a better-suited alternative bearing surface than other designs with regards to strain shielding, bone deformation and bone remodelling.

Thickness of the acetabular component played a crucial role in the implant induced bone remodelling.

(Refer Slide Time: 42:31)

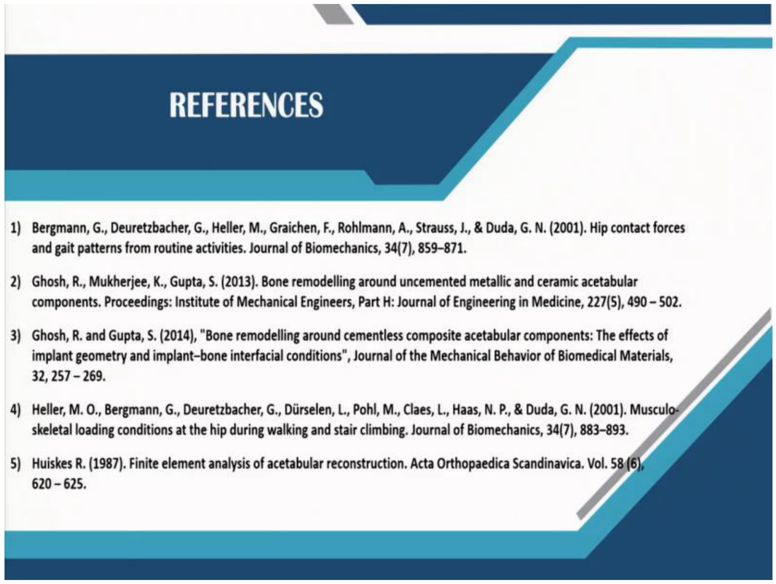

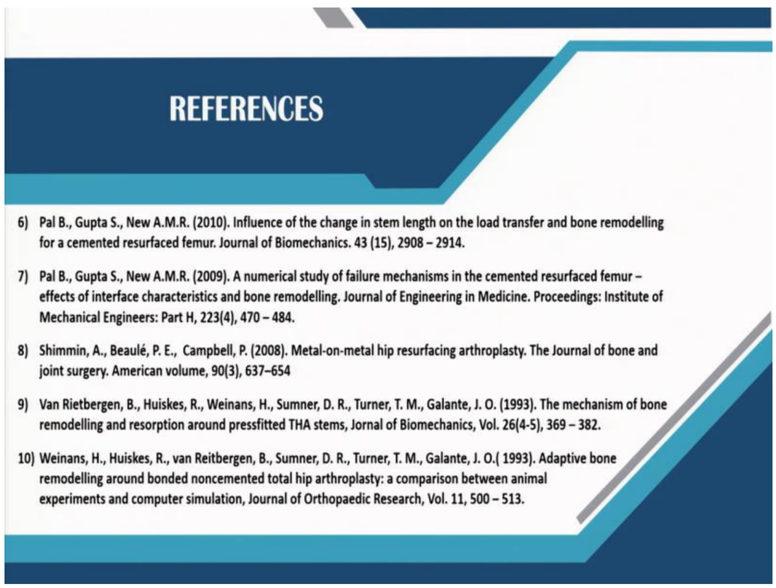

The list of references are included in two slides based on which the lecture has been prepared. Thank you for listening.